4052–4063 *Nucleic Acids Research, 2012, Vol. 40, No. 9* *Published online 11 January 2012*
doi:10.1093/nar/gkr1285

A novel phage-encoded transcription antiterminator acts by suppressing bacterial RNA polymerase pausing

Zhanna Berdygulova[1], Daria Esyunina[2,3], Nataliya Miropolskaya[2], Damir Mukhamedyarov[1], Konstantin Kuznedelov[1], Bryce E. Nickels[1,4], Konstantin Severinov[2], Andrey Kulbachinskiy[2,*] and Leonid Minakhin[1,*]

[1]Waksman Institute of Microbiology, Piscataway, NJ 08854, USA, [2]Institutes of Molecular Genetics and Gene Biology, Russian Academy of Sciences, Moscow 119991, [3]Molecular Biology Department, Biological Faculty, Moscow State University, Moscow 119991, Russia and [4]Department of Genetics, Rutgers, The State University of New Jersey, Piscataway, NJ 08854, USA

Received October 11, 2011; Revised November 28, 2011; Accepted December 14, 2011

ABSTRACT

Gp39, a small protein encoded by *Thermus thermophilus* phage P23–45, specifically binds the host RNA polymerase (RNAP) and inhibits transcription initiation. Here, we demonstrate that gp39 also acts as an antiterminator during transcription through intrinsic terminators. The antitermination activity of gp39 relies on its ability to suppress transcription pausing at poly(U) tracks. Gp39 also accelerates transcription elongation by decreasing RNAP pausing and backtracking but does not significantly affect the rates of catalysis of individual reactions in the RNAP active center. We mapped the RNAP-gp39 interaction site to the β flap, a domain that forms a part of the RNA exit channel and is also a likely target for λ phage antiterminator proteins Q and N, and for bacterial elongation factor NusA. However, in contrast to Q and N, gp39 does not depend on NusA or other auxiliary factors for its activity. To our knowledge, gp39 is the first characterized phage-encoded transcription factor that affects every step of the transcription cycle and suppresses transcription termination through its antipausing activity.

INTRODUCTION

Bacterial RNA polymerase (RNAP) is a complex molecular machine whose activities are tightly regulated by interplay of *cis*-encoded template-specific signals and *trans*-acting transcription factors. While the frequency of transcription initiation is largely determined by promoter recognition, the actual expression level of each gene also depends on the rate of transcription elongation and transcription termination efficiency.

Transcription termination in bacteria may be factor independent (intrinsic) or require specific factors such as Rho or Mfd (1,2). Intrinsic transcription terminators consist of a GC-rich stem–loop (hairpin) in nascent RNA followed by a 7–10 nt U-rich sequence. During intrinsic termination, RNAP first pauses at a U-track, allowing a hairpin to form in the nascent transcript. While normal transcription elongation complexes (TECs) are exceedingly stable, the hairpin destabilizes the TEC, leading to its dissociation. The mechanism(s) responsible for TEC destabilization at terminators are not precisely known and may involve hairpin-induced shearing of the RNA–DNA hybrid, hypertranslocation of RNAP without nucleotide addition, or hairpin invasion into the RNAP main cleft resulting in RNA–DNA melting (2). The termination hairpin may also induce allosteric changes leading to opening of the RNAP main cleft (3).

Transcription antitermination is a widespread regulatory mechanism that allows transcription through terminators and thus controls expression of downstream genes in bacterial operons (4). The best-studied examples of transcription antitermination factors come from analysis of transcription regulation during bacteriophage infection. The *Escherichia coli* phage λ Q protein binds a *qut* site at a late promoter of the phage and modifies host

*To whom correspondence should be addressed. Tel: +7 499 196 00 15; Fax: +7 499 196 00 15; Email: akulb@img.ras.ru
Correspondence may also be addressed to Leonid Minakhin. Tel: +732 445 3688; Fax: +732 445 5735; Email: minakhin@waksman.rutgers.edu

The authors wish it to be known that, in their opinion, the first two authors should be regarded as joint First Authors.

RNAP at a promoter-proximal σ^{70}-dependent pause site. The Q-containing TEC is able to bypass multiple transcription terminators, allowing transcription of late phage genes. The antitermination activity of Q is stimulated by cell-encoded protein NusA (1,4). Phage λ N protein is recruited to the TEC through interaction with a specific *nut* site in the nascent RNA transcript. The effect of N protein alone on transcription termination efficiency is not high, probably because it does not bind the TEC tightly. However, in the presence of host proteins NusA, NusB, S10 and NusG, the N-modified TEC is capable of efficient processive transcription antitermination (1,4). Curiously, NusA on its own increases termination efficiency and stimulates transcription pausing (1,5). In contrast, *E. coli* NusG increases the rate of RNA elongation and suppresses pausing (1,6). RfaH, a specialized NusG paralog, stimulates transcription of horizontally acquired operons in *E. coli* and related bacteria by suppressing RNAP pausing and termination (7,8). Both Q and N also possess an antipausing activity (9–11). Therefore, it was proposed that antiterminator and antipausing proteins may utilize common strategies for TEC modification (8).

Q was found to bind the β flap domain of RNAP, which forms a part of the RNA exit channel (12). The binding site for N is unknown but could also be located close to the β flap (1,4). NusA was shown to interact with the α-subunit C-terminal domains (αCTDs) and additional RNAP elements near the RNA exit channel including the β flap (5,13). The binding sites for NusG and RfaH are found in the β′ clamp helices at the DNA-binding cleft of RNAP (14,15). RfaH can simultaneously interact with the β gate loop at the opposite side of the DNA-binding cleft, physically locking the nucleic acids inside the cleft and thus stabilizing TECs at terminators (16). The binding site for p7, an antiterminator protein encoded by *Xanthomonas oryzae* phage Xp10, is located near the N-terminal Zn finger domain in the largest RNAP subunit β′ (17). Overall, it appears that known antitermination (and termination) factors interact with the 'upstream face' of RNAP in the TEC, close to the RNA–DNA hybrid and nascent RNA that exits the complex. From this location, these proteins may affect the conformation of the nascent transcript and/or its interactions with RNAP or DNA, changing the elongation properties of the enzyme.

RNAPs from thermophilic bacteria *Thermus thermophilus* (*Tth*) and *Thermus aquaticus* (*Taq*) represent an attractive model to study transcription antitermination due to availability of 3D structures of free RNAP and various transcription complexes (18–21). However, no antitermination factors acting on these enzymes are currently known. Previously, we reported that gp39 protein encoded by *Tth* phage P23–45 binds *Tth* RNAP and inhibits transcription initiation from host bacterial promoters *in vitro* (22). Here, we demonstrate that gp39 also stimulates elongation and acts as an antiterminator during transcription at intrinsic terminators. We define the mechanism of gp39-dependent transcription antitermination and map the gp39 interaction site on RNAP. Our results open the way for a detailed structural understanding of transcription termination/antitermination, the least understood parts of the transcription cycle.

MATERIALS AND METHODS

Proteins

Escherichia coli strains XL-1Blue and BL21(DE3) were used for molecular cloning and recombinant protein expression, respectively. DNA fragments encoding gp39 and *Tth* NusA were cloned into pET28a, expressed in *E. coli* and purified as N-terminal 6His-tagged fusions by affinity chromatography on Ni-NTA agarose column (GE Healthcare) followed by ion-exchange chromatography on MonoQ column (GE Healthcare). The 6His-tag was removed from gp39 by thrombin cleavage followed by affinity chromatography on Ni-NTA agarose column to separate the untagged gp39 and the histidine tag. *Tth* RNAP core and holoenzymes with the C-terminally 10His tagged β′-subunit were purified from the *Tth* HB8rpoC::10 H strain as described in (23). Wild-type and mutant *Taq* core RNAPs were purified from *E. coli* BL21(DE3) cells coexpressing all four core RNAP subunits essentially as described in (24,25). *Taq* and *Tth* N-terminal 6His-tagged σ^A-subunits were expressed in BL21(DE3) and purified as described in (26) and (23), respectively.

Bacterial two-hybrid assay

Escherichia coli strain FW102 O_L2-62 (27) containing the *lacZ* gene under the control of test promoter p*lac*O_R2-62 on an F′ episome was used in the bacterial two-hybrid assay. Plasmids for two-hybrid analysis encoding for gp39 and *Tth* β flap gene fusions were created by cloning of corresponding PCR fragments between the NotI and BamHI sites of the plasmids pBRαLN, encoding for the N-terminal domain (NTD) of the RNAP α-subunit, and pACλCI32, encoding for the DNA-binding domain of the λCI protein, as described in (28). The measurements of β-galactosidase activity were performed as described (29). Control experiments were performed using the parent vector plasmids (negative controls).

Native gel-binding assay

Either the wild-type or mutant Δflap *Taq* core RNAPs (1 μM) were mixed with *Taq* σ^A (2 μM, where indicated) and/or gp39 (5 μM) in 10 μl of transcription buffer and incubated for 10 min at 55°C. About 5 μl of the reaction mixture was resolved on a native 4–15% (w/v) Phast gradient polyacrylamide gel (GE Healthcare). Protein bands were visualized by Coomassie blue staining, excised from the native gel and placed into the wells of a gradient 12–16% (w/v) polyacrylamide denaturing SDS gel, followed by electrophoresis and silver staining.

In vitro transcription assays

Promoter-terminator fusion DNA templates were obtained by PCR from P23–45 genomic DNA, from

plasmids containing corresponding sequences or from synthetic oligonucleotides. For analysis of transcription termination by wild-type RNAP, TECs halted at position +20 of the T7 A1 promoter templates (Supplementary Figure S1) were prepared by performing transcription initiation with *Tth* or *Taq* RNAP σ^A holoenzymes in the presence of a limited substrate set: 200 μM CpApUpC, 20 μM ATP, 10 μM CTP, 10 μM GTP (with addition of [α-^{32}P] GTP). The reactions were performed in transcription buffer containing 20 mM Tris–HCl, pH 7.9, 40 mM KCl and 10 mM $MgCl_2$ for 5 min at 55°C and placed on ice. To prevent reinitiation, heparin was added to 0.05 mg/ml. Transcription termination by the Δβ flap tip and ΔαCTD mutant RNAPs was analyzed using a DNA template that contained an extended −10 promoter, *gal*P1, fused to the tR2 terminator (Supplementary Figure S1). To study transcription termination and antitermination at various conditions, aliquots of the halted TECs were supplemented with gp39 and/or NusA, and the reactions were incubated for 5–10 min at specific conditions indicated in figure legends, followed by addition of NTPs. The reactions were stopped after indicated time intervals by addition of equal volume of urea–formamide loading buffer.

Analysis of the elongation rate of *Tth* RNAP was performed on a PCR template containing the λP_R promoter (Supplementary Figure S1) fused to a 600-bp-long fragment of the *E. coli rpo*B gene from pIA146. Stalled TECs containing radioactively labeled 26-nt-long RNA were prepared by performing transcription initiation with *Tth* RNAP σ^A holoenzyme in the presence of 100 μM ApU, 5 μM ATP, 5 μM GTP, 1 μM UTP (with addition of [α-^{32}P] UTP). Transcription was restarted by the addition of NTPs and transcript elongation was monitored at 55°C either in the absence or in the presence of gp39. Analysis of nucleotide addition in complex of *Tth* RNAP with the minimal scaffold template was performed essentially as described previously (30). Gp39 was added to 5 μM 5 min before nucleotides. The reaction of pyrophosphorolysis was performed at 40°C in the presence of 5 mM pyrophosphate as described (30). Analysis of RNA cleavage in reconstituted TECs containing 13-mer RNA was performed as described in ref. (30). The TEC was assembled in the absence of Mg^{2+} ions, gp39 was added to 10 μM, the samples were incubated for 3 min at 37°C, $MgCl_2$ was added to 10 mM and the cleavage kinetics was monitored.

Analysis of transcription termination in reconstituted TECs

TEC reconstitution on the nucleic acid scaffold corresponding to the t65 terminator was performed using *Tth* core RNAP and the DNA and RNA oligonucleotides shown on Figure 4A. Template DNA oligonucleotide (2.5 μM) was incubated with RNA (250 nM, 5′-end labeled with γ-^{32}P-ATP and T4 polynucleotide kinase) in buffer containing 40 mM Tris–HCl pH 7.9 and 40 mM KCl for 5 min at 65°C and cooled to 20°C. The samples were diluted 3-fold, core RNAP was added to 250 nM and the samples were incubated for 10 min at 37°C. Non-template DNA oligonucleotide was added to 2 μM, and incubation was continued for another 20 min. The reconstituted TECs were bound to Ni-NTA agarose beads (Qiagen), followed by washing of the beads with 1 ml of buffer containing 40 mM Tris–HCl pH 7.9 and 500 mM KCl and with 3 × 1 ml of buffer containing 250 mM KCl (for analysis of full-length RNA synthesis) or 100 mM KCl (for analysis of RNA release in stalled TECs).

For analysis of oligonucleotide-mediated termination, antisense oligonucleotides ('−11' or '−15', 10 μM), $MgCl_2$ (10 mM) and NTPs (25 μM) were added and transcription was performed at 50°C. Gp39 (10 μM) and NusA (500 nM) were added 3 min prior to oligonucleotide addition, when indicated. After 10 min, the reactions were divided into supernatant and pellet fractions; the pellet fractions were briefly washed with 200 μl of the transcription buffer to remove residual RNAs that were released into solution. The efficiency of termination was calculated as the amount of RNAs released into the supernatant fraction at the point of terminator (30–33 nt RNAs) divided by the total amount of RNAs ≥30 nt in both the supernatant and the pellet fractions. For analysis of oligonucleotide-mediated RNA release in stalled TECs, the starting 23-mer TEC was elongated to 33-mer TEC in the presence of UTP and CTP (10 μM) and antisense oligonucleotides (10 μM) and incubated for 10 min at 50°C either in the absence or in the presence of gp39, followed by separation of the supernatant and pellet fractions. Analysis of RNA cleavage with RNase H (0.5 U/10 μl reaction point) was performed at 37°C in stalled 33-mer TEC in the presence of the '−15' oligonucleotide (10 μM).

σ^A-dependent pausing assay

The detailed conditions of the σ-dependent pausing assay in reconstituted TECs are described in (42). Briefly, the TECs were reconstituted from *Tth* core RNAP and DNA and RNA oligonucleotides shown on Figure 6A in the same way as in the case of the t65 terminator scaffold, and the σ^A-subunit was added to 1 μM. Reconstituted TECs were sorbed to Ni-NTA agarose, and transcription was performed at 37°C in the presence of 100 μM NTPs in transcription buffer containing 40 mM Tris–HCl pH 7.9, 40 mM KCl and 10 mM $MgCl_2$. Gp39 was added to 10 μM 3 min before addition of NTPs.

RESULTS

Gp39 antiterminates transcription by *Tth* RNAP at intrinsic terminators

Analysis of *in vitro* transcription by *Thermus* (*Tth* or *Taq*) RNAP in the presence of gp39 revealed, unexpectedly, that gp39 suppresses transcription termination (Figure 1; our unpublished data). To study this phenomenon, we analyzed *Thermus* RNAP transcription from four templates containing different intrinsic terminators with different hairpin stem lengths (ranging from 8 to 21 bp) and loop sizes (ranging from 3 to 10 nt) (Figure 1A). Two terminators tested, phage λ tR2 and tR′, are classic

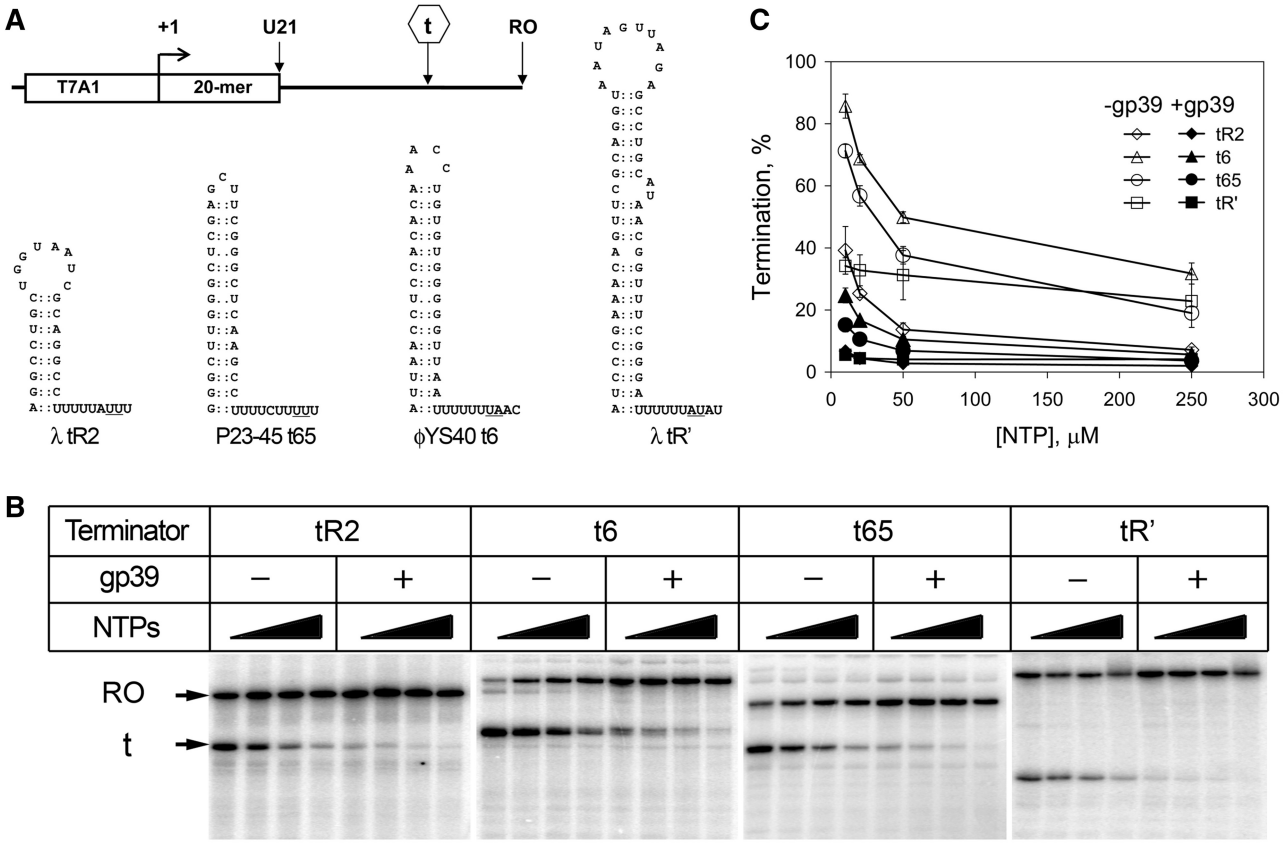

Figure 1. Gp39-mediated transcription antitermination by *Tth* RNAP at different intrinsic terminators. (**A**) The scheme of the terminator constructs shows positions of the transcription start site (+1), 20-nt-long U-less region, termination site (t) and the run-off (RO) transcript. The sequences of the terminators are shown below the scheme; the transcript release points are underlined. (**B**) Termination was assayed after addition of NTPs (10, 25, 50 or 250 μM) to stalled U21 TECs in the absence or in the presence of gp39. (**C**) Plot shows termination efficiencies at different NTP concentrations. The plot shows averages and standard deviations from three independent experiments.

model terminators used to study *E. coli* RNAP termination; two others, t65 from *Tth* phage P23–45 and t6 from *Tth* phage ϕYS40 (23), were predicted based on sequence analysis. Each terminator was fused to the T7 A1 promoter, which allowed the preparation of stalled TECs containing 21-nt-long radiolabeled RNA, followed by addition of gp39 and unlabeled NTPs (see 'Materials and Methods' section for details).

All four terminators were recognized by *Tth* RNAP (Figure 1B and C). On three terminators, termination efficiencies significantly decreased with increasing NTP concentrations (from 86% at 10 μM NTPs to 32% at 250 μM at the strongest terminator t6, and from 40% to 7% at the weakest terminator tR2). In contrast, the termination at the tR′ terminator only weakly depended on NTP concentrations. Gp39 significantly decreased termination at each terminator at every NTP concentration tested (Figure 1B and C). The degree of antiterminaton effect of gp39 was similar at different NTP concentrations; the read-through fraction in the presence of gp39 was highest at high NTP concentrations and lowest at low NTP concentrations, when significant termination was observed even in the presence of gp39 (Figure 1C). The antitermination activity of gp39 was observed at a wide range of conditions, including variations in the ionic strength (from 50 to 450 mM KCl in the reaction buffer, Supplementary Figure S2A) and the reaction temperature (from 37°C to 55°C, Supplementary Figure S2B).

Gp39 overcomes NusA-induced transcription termination

The antitermination activities of λ phage antiterminators N and Q depend on NusA (see 'Introduction' section). We analyzed the effect of recombinant *Tth* NusA on transcript termination on tR2 and t65 in the presence or in the absence of gp39. In the presence of 25 μM NTPs and NusA, termination efficiencies on both terminators reached ~100% (Figure 2A, lanes 4 and 5), compared to 25% for tR2 and 50% for t65 in the absence of NusA (Figure 2A, lane 1). The half termination-stimulatory concentration of NusA was <25 nM (Supplementary Figure S3A). Gp39 fully suppressed the effect of NusA and stimulated efficient terminator read-through (compare lanes 2, 3 and 6, 7 in Figure 2A). While the Q protein of lambdoid phage 82 (Q^{82}) efficiently antiterminates at elevated NTP concentrations, it still requires NusA for antitermination at low NTP concentrations, when termination is more efficient (11). We therefore repeated the experiment with the tR2 terminator using low NTP

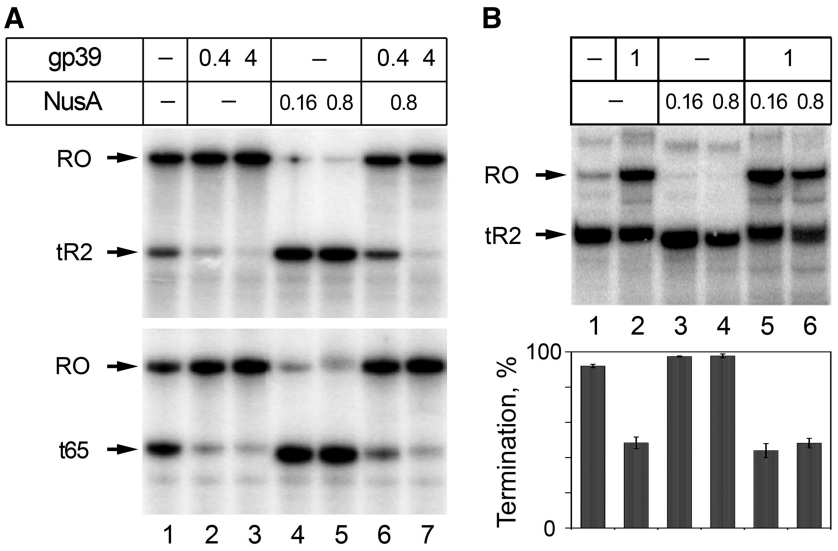

Figure 2. Analysis of the NusA effects on intrinsic termination and gp39-mediated antitermination. (**A**) Analysis of termination on the λtR2 (top) and t65 (bottom) terminators in the presence of gp39 (0.4 and 4 μM) and NusA (0.16 and 0.8 μM). Transcription was performed at 25 μM NTPs. (**B**) NusA effects on gp39-mediated antitermination at low NTP concentrations (2.5 μM). Gp39 and NusA were present at 1 μM and 0.16/0.8 μM. The plot shows averages from two independent experiments.

concentrations (2.5 μM) (Figure 2B). Under these conditions, the efficiency of intrinsic termination reached 92%; NusA increased it to 98% while gp39 decreased the level of termination to ~50% irrespective of the presence or the absence of NusA.

To analyze possible interplay between the two factors in more detail, we compared the concentration dependence of the antitermination effect of gp39 in the absence and in the presence of NusA (taken at 50 nM) (Supplementary Figure S3). NusA partially suppressed gp39-mediated antitermination at low gp39 concentrations. However, gp39 efficiently antiterminated at concentrations >100 nM and NusA did not significantly decreased the level of antitermination at these conditions (Supplementary Figure S3A and S3B). Overall, these results suggest that the antitermination effect of gp39 does not significantly depend on NusA and gp39 overrides the stimulatory effect of NusA on termination. The results suggest that gp39 may either directly prevent RNAP interaction with NusA, or allosterically change the conformation of the TEC, making it resistant to NusA action.

Gp39 interacts with RNAP through the β flap domain

To identify what surface of RNAP is contacted by gp39, we analyzed several *Taq* RNAP mutants harboring extensive deletions, (i) the β flap tip deletion (Δ757–793); (ii) the *Thermus*-specific β′ non-conserved domain (β′NCD) deletion (Δ159–451); and (iii) deletion of the αCTD (Δ231–315). *Taq* RNAP mutants with deletions of the β flap tip and αCTDs are unable to efficiently recognize −10/−35 promoters (24). Thus, to test termination by these RNAP mutants we used a DNA template that contained an extended −10 promoter, *gal*P1, fused to the tR2 terminator. Whereas deletion of the β′NCD or αCTDs had no major effect on gp39 activity (Supplementary Figure S4), deletion of the β flap completely eliminated the ability of gp39 to antiterminate transcription (Figure 3A). Thus, we conclude that the β flap tip is essential for gp39-mediated antitermination.

To determine whether the β flap tip contains a binding site for gp39, we performed native gel-binding experiments with the wild-type and the Δβ flap tip *Taq* RNAPs (Supplementary Figure S5). Gp39 affected the native gel electrophoretic mobilities of wild-type core and holoenzyme but did not change the mobilities of the mutant RNAP. Analysis of protein composition of RNAP bands excised from the gel demonstrated that gp39 interacts with the wild-type RNAPs but not with the Δβ flap RNAPs, suggesting that the *Thermus* RNAP β flap likely harbors a gp39-binding site (Supplementary Figure S5).

To localize the gp39-binding site in the β flap we used a bacterial two-hybrid assay (31). In this assay, contact between a protein domain fused to a component of RNAP (here, the α-subunit) and a partner protein fused to a DNA-binding protein (here, the CI protein of λ) activates transcription of a *lacZ* reporter gene under the control of a test promoter bearing an upstream recognition site for the DNA-binding protein (here, a λ operator). The *Tth* RNAP β flap domain was fused to the α-subunit NTD, replacing the αCTD, and gp39 was fused to λCI. First, we tested the interaction of gp39 with the entire *Tth* β flap domain (residues 703–830) and detected high level of β-galactosidase activity, confirming gp39—β flap interaction (Figure 3B). To test if gp39 interacts with the flap tip helix as Q protein does (12), we next constructed a deletion of the central part of the β flap removing the tip helix (Δ762–786); the removed amino acid were replaced with three alanines to minimize structural perturbations. The plasmid expressing the β flap fusion with this deletion provided high level of β-galactosidase

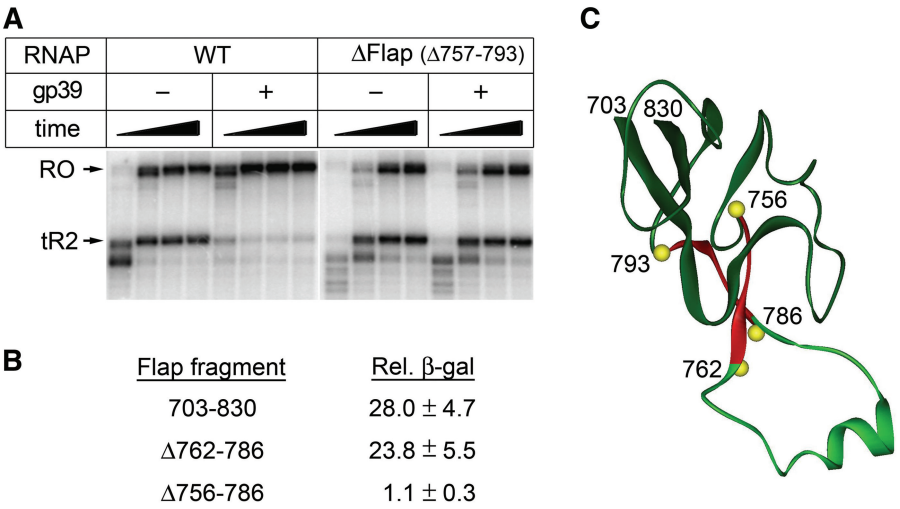

Figure 3. Gp39 targets the β flap domain of *Thermus* RNAP. (**A**) Analysis of the effects of gp39 on transcription termination by wild-type (WT) and Δβ flap *Taq* RNAPs at the λtR2 terminator. Transcription was performed at 25 μM NTPs. (**B**) Mapping of the gp39 interaction site in the β flap domain of *Tth* RNAP by a bacterial two-hybrid assay. The numbers at the right indicate the β-galactosidase activity measured in Miller units relative to the negative control and represent average values and standard deviations from at least three independent experiments. (**C**) The β flap domain structure [*Tth* TEC, 2O5I (21)].The positions of the analyzed deletions are indicated. The flap tip region (amino acids 762–786) is shown in light green.

activity comparable to those seen with the plasmid expressing the entire β flap domain suggesting that gp39 utilizes the binding locale other than Q (Figure 3B). In contrast, deletion of a larger β flap segment (Δ756–786) abolished the β flap-gp39 interaction in the two-hybrid assay (Figure 3B), in agreement with the absence of gp39 interaction with the Δβ flap RNAP (Figure 3A). Further analysis is required to establish whether the deleted segment includes the binding site for gp39 or the deletions structurally change the gp39-β flap interface. However, the results strongly suggest that the gp39-binding site is located within the β flap domain and that it does not include the distal part of the β flap tip.

Gp39 suppresses oligonucleotide-mediated termination and decreases RNAP pausing at terminators

During intrinsic termination RNAP first pauses at the terminator U-track, after which termination hairpin formation leads to disruption of the TEC (see 'Introduction' section). Thus, gp39 could suppress intrinsic termination by suppressing U-track-dependent pausing, by preventing RNA hairpin formation, or by stabilizing the TEC and making it more resistant to hairpin-induced changes. To better understand the antitermination mechanism of gp39, we used an oligonucleotide-mediated termination assay (32). In this assay, the upstream part of the terminator hairpin is removed from the DNA template and RNA release from the TEC at the normal termination point is induced by the addition of a DNA oligonucleotide complementary to the nascent RNA and mimicking the missing upstream part of the terminator hairpin. A nucleic acid scaffold based on the t65 sequence was used in the experiments (Figure 4A). The 23-nt-long RNA included the downstream part of the terminator hairpin and had a 3′-end located just before the 10-nt-long U-track. To reveal RNA transcripts released into solution as a result of termination, we performed *in vitro* transcription reactions with *Tth* RNAP immobilized on Ni-NTA agarose and separated the supernatant and agarose-bound fractions upon the completion of the reaction. In the absence of complementary oligonucleotide, most RNAP molecules transcribed to the end of the template generating a 58-nt-long runoff product, with only ~10% of total RNA being released into solution at t65 termination sites (correspond to RNA lengths of 30–33 nt, Figure 4B, lanes 2 and 3). In the presence of a 15-nt-long antisense DNA oligonucleotide, whose 5′-end was located 11 nt upstream of the end of the U-track ('−11' oligonucleotide), the efficiency of release of 30–33 nt RNA products increased to ~33% (lanes 6 and 7), with majority of termination events occurring at the eighth and ninth nucleotides of the U-track (31 and 32 nt RNAs, correspondingly). Importantly, oligonucleotide '−15' that annealed four nucleotides upstream of the '−11' oligonucleotide, did not stimulate RNA release (lanes 10 and 11), an expected result since complementary oligonucleotide should be located no farther than 11 nt from the termination point to cause efficient RNA release (11). We conclude that this synthetic scaffold-based oligonucleotide release assay is an appropriate system to study termination by *Tth* RNAP. We next tested the effects of gp39 on RNA release. In the absence of added oligonucleotides, gp39 did not have any significant effect on transcription (Figure 4B, lanes 4 and 5). However, gp39 efficiently suppressed the '−11' oligonucleotide-mediated RNA release (compare lanes 7 and 9). Thus, the effects of gp39 on transcription termination are fully reproduced in this system.

To test gp39 effects on transcription pausing at the terminator, we analyzed RNA synthesis on the scaffold template at 37°C, a suboptimal temperature that slows *Tth* RNAP, and used shorter incubation times and lower

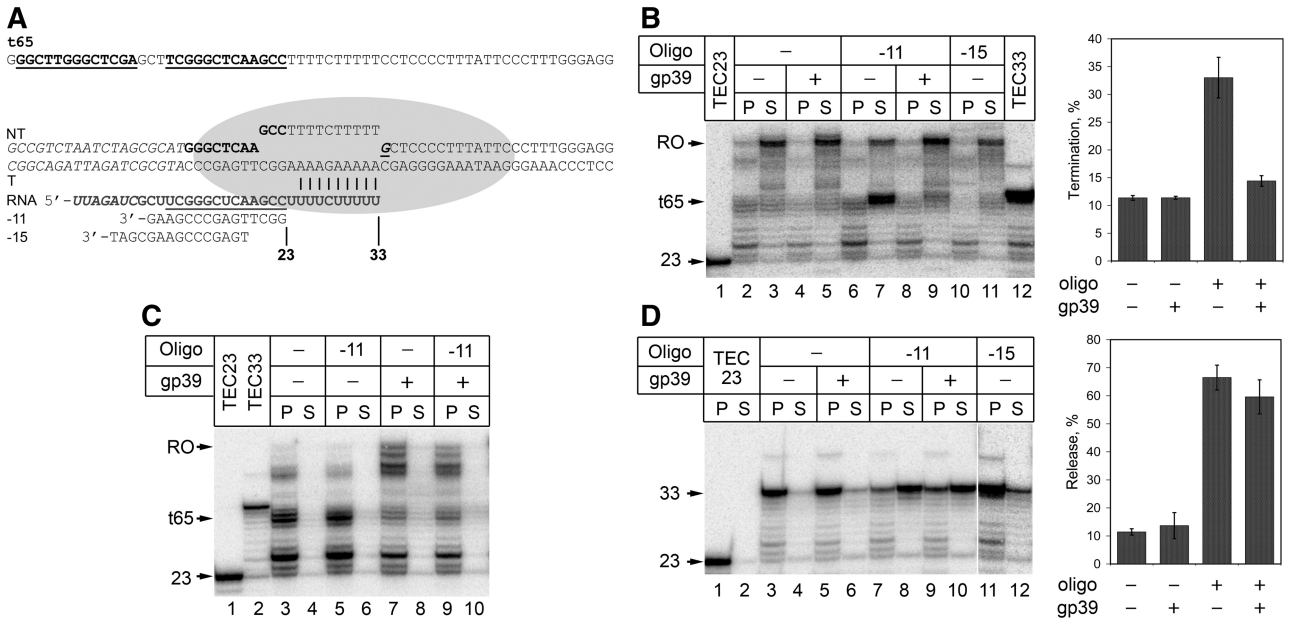

Figure 4. Analysis of gp39 activity in the oligonucleotide-mediated termination assay. (**A**) Synthetic scaffold template used in the experiments (NT, non-template DNA strand; T, template DNA strand); the sequences that were changed in comparison with the wild-type t65 terminator are shown in italics. The t65 sequence is shown at the top; the upstream and the downstream parts of the terminator hairpin stem are bold underlined. RNA 3′-end positions in the starting 23-mer and in the stalled 33-mer TECs are indicated below the RNA sequence. The '−11' and '−15' DNA oligonucleotides used for RNA release are shown below the scaffold. (**B**) Oligonucleotide-mediated termination assay. The starting 23-mer TEC was elongated in the presence of all four NTPs either in the absence or in the presence of oligonucleotides '−11', '−15' and gp39; the resulting reactions were separated into pellet (P) and supernatant (S) fractions and analyzed by PAGE. The plot on the right shows termination efficiencies calculated as the amount of 30-33 nt RNAs released into the S fraction divided by the total amount of ≥30 nt RNAs in both S and P fractions (the data from three independent experiments). (**C**) Analysis of gp39 antipausing activity during transcription on the scaffold template. (**D**) RNA release in stalled 33-mer TEC in the presence of oligonucleotides '−11' and '−15' and gp39. The plot shows the efficiencies of RNA release.

NTP concentrations (1 min incubation and 10 μM NTPs instead of 10 min incubation and 25 μM NTPs used in the previous experiment). Under these conditions, the TEC paused when the RNA length reached 30–32 nt, at positions corresponding to points of RNA release. Efficient pausing was observed both in the presence and in the absence of the '−11' oligonucleotide (Figure 4C, lanes 3–6) indicating that the U-track induces pausing in the absence of the termination hairpin. RNA from paused *Tth* RNAP TECs was not efficiently released into solution at these conditions (lanes 4 and 6), likely as a result of increased TEC stability at low temperatures and slow kinetics of oligonucleotide-mediated RNA release. Similarly, only minor RNA release was observed previously at the same incubation time at 37°C with *E. coli* RNAP (11). Gp39 significantly decreased pausing and stimulated read-through; this effect was observed both in the absence and in the presence of the antisense oligonucleotide (lanes 7–10). The result suggests that gp39-induced suppression of pauses may play a significant role in the antitermination mechanism.

Gp39 does not stabilize the TEC at the termination site and does not protect nascent RNA

To test whether gp39 stabilizes the TEC at terminators, we analyzed RNA release in TECs stalled at the end of the t65 U-track. The stalled TECs containing a 33-nt-long transcript were obtained by 'walking' the starting 23-mer TEC in the presence of UTP and CTP. In the absence of antisense oligonucleotides, these TECs were stable, and only small amounts of 33-mer RNA were released into solution (Figure 4D, lanes 3–6). The addition of the '−11' oligonucleotide strongly stimulated TEC dissociation, with ~65% of RNA released after 10 min (lanes 7 and 8). The control '−15' oligonucleotide did not stimulate RNA release (lanes 11 and 12). Remarkably, gp39 did not significantly decrease the efficiency of RNA release (Figure 4D, lanes 9 and 10 and plot on the right). Furthermore, gp39 did not change the kinetics of RNA release (Supplementary Figure S6). Thus, gp39 did not stabilize the TEC stalled at the termination point, at least under the conditions of the oligonucleotide-mediated RNA release assay. These results suggest that gp39-mediated antitermination is unlikely to proceed via stabilization of the TEC.

The inability of gp39 to inhibit oligonucleotide-mediated RNA release in stalled TECs suggested that it does not affect accessibility of nascent RNA. To directly test this notion, we used an RNase H protection assay previously developed by Roberts and co-workers (11). In this assay, the RNA accessibility is probed by annealing of complementary DNA oligonucleotides whose 5′-ends are positioned >11 nt upstream from the RNA 3′-end and which do not cause TEC dissociation, followed by RNase H digestion. RNA in the 33-mer TEC stalled at the end of the terminator was resistant to RNase H

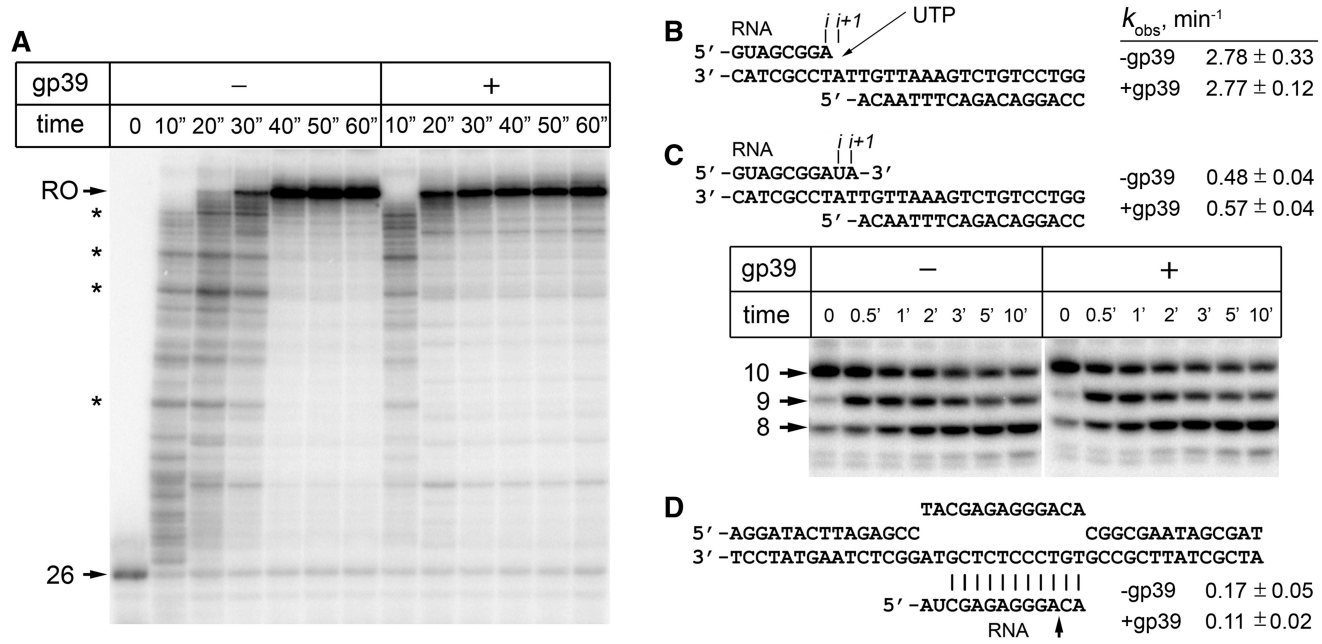

Figure 5. Influence of gp39 on transcription elongation by *Tth* RNAP. (**A**) Analysis of the average elongation rates of *Tth* RNAP on the λP_R-*rpoB* template. Positions of the starting 26-mer and full-length run-off transcripts are indicated at the left; positions of several transcription pauses are indicated with asterisks. (**B**) Analysis of the rates of single nucleotide addition in complex of *Tth* RNAP with the minimal nucleic acid scaffold. (**C**) Effect of gp39 on the reaction of pyrophosphorolysis. Positions of the starting 10 nt RNA and 8/9 nt reaction products are shown on the left of the gel. The apparent k_{obs} values (min^{-1}) correspond to the rates of accumulation of the 8 nt RNA product. (**D**) Effect of gp39 on the reaction of intrinsic endonucleolytic RNA cleavage. The cleavage site of RNA in the synthetic scaffold is indicated by an arrow.

(Supplementary Figure S7, lanes 1 and 2). In the presence of the '−15' DNA oligonucleotide, RNA was progressively cleaved indicative of the formation of the RNA–DNA hybrid that was targeted by RNase H (lanes 3–5). Gp39 did not have any effect either on the pattern or kinetics of RNA digestion in the presence of the oligonucleotide (lanes 7–9). The protection of nascent RNA from RNase H digestion by the Q^{82} protein was previously shown to strongly depend on the NusA protein (11). In contrast, *Tth* NusA did not increase RNA protection by gp39 (Supplementary Figure S7, lanes 13–15). Thus, gp39 is unable to prevent oligonucleotide annealing to nascent RNA and is therefore unlikely to antiterminate through preventing RNA hairpin formation.

Gp39 accelerates transcription elongation by reducing transcription pausing

The ability of gp39 to decrease RNAP pausing at the terminator suggested that it may also affect the rate of transcription elongation. To test this notion, we analyzed transcription on a DNA template containing a λ P_R promoter fused to a 600-bp-long DNA fragment from the *rpoB* gene of *E. coli*. The *rpoB* template is devoid of strong pause signals and was previously used for comparison of transcription rates of various RNAPs (30,33). Gp39 increased the average elongation rate of *Tth* RNAP ~2-fold: when transcription was performed at 55°C in the absence of gp39, most RNAPs reached the end of the template after ~40 s, while in the presence of gp39 the reaction was complete by 20 s (Figure 5A). Similar 2-fold stimulatory effects of gp39 were observed when transcription was repeated at low temperatures at which the transcription rate of *Thermus* RNAP is significantly reduced (Supplementary Figure S8). Gp39 also significantly decreased the duration of transcription pauses (indicated with asterisks on Figure 5A) that were observed at several positions of this template. Thus, gp39 exhibits antipausing activity during both transcription elongation and termination and increases the average elongation rate.

The observed effect of gp39 suggested several possible modes of its action. In particular, gp39 might increase the catalytic rate of RNAP, affect TEC translocation or prevent isomerization of TEC into a paused state and/or TEC backtracking. We first analyzed the effect of gp39 on nucleotide addition, using a minimal scaffold template that was previously shown to bind *Thermus* RNAP in an active post-translocated conformation (Figure 5B) (30). The measurements were performed at saturating substrate concentration (1 mM UTP) but at a low (10°C) temperature to allow manual mixing of reagents. The rates of nucleotide addition were found to be identical in the absence or in the presence of gp39 (Figure 5B). Thus, the antipausing activity of gp39 cannot be explained by its effect on the rate of catalysis of nucleotide addition in the RNAP active center. Next, we tested the effect of gp39 on TEC translocation by determining whether gp39 affects the rate of pyrophosphorolysis, the reversal of the nucleotide addition reaction, which occurs in the pre-translocated TEC conformation. As shown in Figure 5C, gp39 did not significantly change the rate of the pyrophosphorolysis, measured on a minimal template

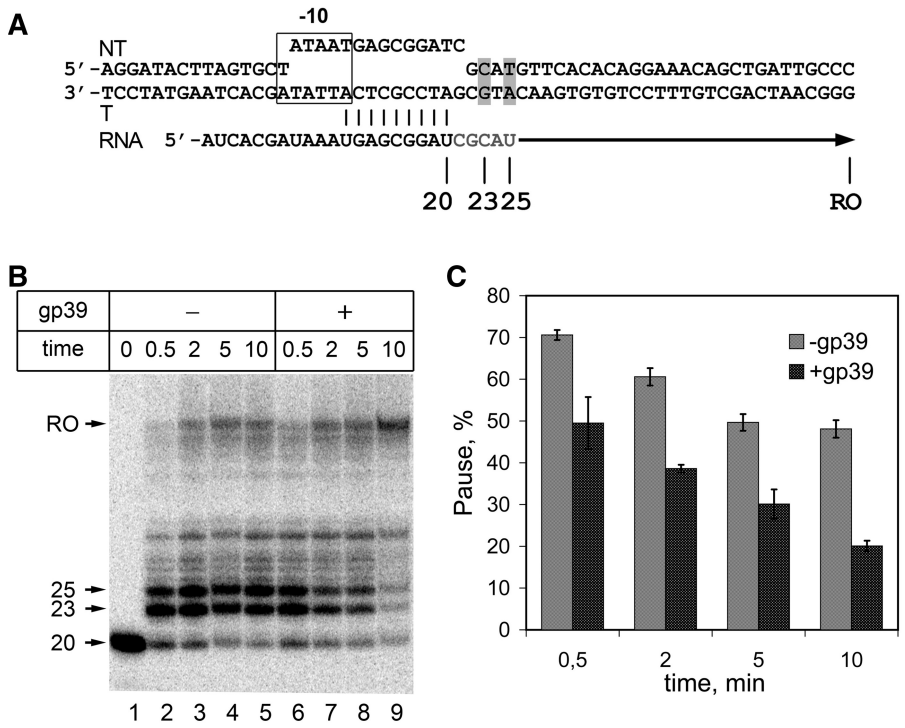

Figure 6. Effect of gp39 on σ^A-dependent pausing. (**A**) The scheme of the nucleic acid scaffold used for analysis of σ^A-dependent pausing. The −10-like pause-inducing sequence is boxed, RNA 3′-end positions in the starting 20-mer, paused and full-length transcripts are indicated below the scheme. (**B**) Analysis of σ^A-dependent pausing in the absence or in the presence of gp39. (**C**) The plot showing the pause efficiencies (the data from three independent experiments).

that was previously shown to be prone to pyrophosphorolysis (30). Thus, gp39 does not significantly affect the balance between pre- and post-translocation TEC states during catalysis. Finally, we determined whether gp39 affects TEC backtracking, by measuring the rate of intrinsic RNA cleavage by *Tth* RNAP in stalled reconstituted TECs containing 13-mer RNA (Figure 5D). The major cleavage site on this template is located 2 nt upstream from the RNA 3′-end and thus corresponds to 1 nt TEC backtracking (30). Gp39 had a weak (~1.5-fold) inhibitory effect on the rate of RNA cleavage by *Tth* RNAP suggesting that it might suppress RNAP backtracking (Figure 5D). Similar results were obtained for all three reactions on other transcription templates that had different sequence contexts (our unpublished data).

Although *Tth* RNAP poorly responds to *E. coli*-specific hairpin-dependent and backtracking-dependent pauses (33), *Tth* RNAP does efficiently form σ-dependent pauses (33) that depend on interactions of the σ-subunit with a −10-like pause inducing sequence in the non-template DNA strand in the TEC (34,35). σ-Dependent pausing is accompanied by TEC backtracking that significantly increases the pause half-life (35). The observed effects of gp39 on transcription pausing and RNAP backtracking suggested that it may also influence the σ-dependent pausing by *Tth* RNAP. To test this hypothesis, we used a recently developed scaffold-based approach for pause analysis (42). The TEC was assembled on a synthetic scaffold containing a consensus −10-like pause-inducing sequence (Figure 6A), followed by addition of the σ^A-subunit and NTPs in the presence or in the absence of gp39. In the absence of gp39, *Tth* RNAP efficiently paused after addition of 3 and 5 nt to the initial 20 nt RNA (Figure 6B). The pausing efficiency reached 70% and the pause half-life exceeded 10 min (Figure 6C). Gp39 significantly decreased both the pause half-life and the fraction of TECs that paused (Figure 6B and C). Thus, gp39 can stimulate transcription through the pause site and even reactivate the paused TECs.

DISCUSSION

In this work, we demonstrated that gp39, a small 16.2 kDa protein encoded by *Tth* phage P23–45 with no similarity to known proteins from public databases (22), acts as an efficient transcription antiterminator on intrinsic terminators of various origins and stimulates RNA elongation by *Thermus* RNAP. As was demonstrated previously, gp39 can also inhibit transcription initiation by *Tth* RNAP from host bacterial −10/−35 promoters, but not from phage P23–45 middle and late promoters that belong to the extended −10 class (22). Thus, gp39 is a multifunctional transcription regulator that may help redirect transcription by *Thermus* RNAP from host to phage promoters and stimulate expression of the phage middle and late genes through its antitermination activity.

Gp39 binds to the *Thermus* RNAP β flap domain that has emerged as a common target for factors affecting the elongation and termination properties of the TEC. Indeed, a number of elongation, termination and antitermination factors in *E. coli* were shown to bind to β flap (Figure 7, see 'Introduction' section). The β flap is located along the nascent RNA exit pathway and either interacts with or is physically close to RNA hairpins that cause pausing or termination (36,37). The flap is flexibly connected to the RNAP mainframe and its interactions with the nascent transcript may cause it to change its position, inducing long-range allosteric changes in the RNAP active center, which have been proposed to occur during termination (3,36,37). Thus, a factor that binds the β flap may influence every step of the termination process, including RNAP pausing at the terminator, formation of secondary structures in the nascent RNA and induction of long-range rearrangements in the RNAP active center, ultimately leading to RNA : DNA hybrid melting and TEC dissociation.

Our studies demonstrate that gp39 does not stabilize the TEC at the point of termination and does not protect the nascent RNA. However, gp39 does suppress transcription pausing and generally increases the rate of transcript elongation. Thus, gp39 should stimulate the passage of RNAP through the terminator U-track, a point where termination kinetically competes with elongation. Importantly, gp39 does not change the catalytic rates of nucleotide addition and pyrophosphorolysis measured in active non-paused TECs, indicating that the antipausing/antitermination activities of gp39 cannot be explained by a direct effect on the rates of catalysis. Rather, gp39 may allosterically favor the active TEC conformation and suppress RNAP backtracking. In particular, gp39 may prevent the β flap-induced allosteric changes in the RNAP active center (3,36,37) and suppress formation of elemental pauses, the first step in transcription pausing, which is likely accompanied by fraying of the RNA 3′-end in the active center (38,39). Gp39 action may also depend on additional RNAP elements in the RNA exit channel and in the main RNAP cleft, including the β′ lid, zipper and Zn finger domains that are involved in interactions with DNA and RNA (Figure 7).

Previously, it was shown that, in contrast to *E. coli* RNAP, *Tth* RNAP is resistant to pause-inducing signals and is not accelerated by NusG, a factor that promotes forward RNAP translocation and stabilizes the TEC in the active post-translocated conformation. Thus, it was proposed that *Tth* RNAP is a naturally 'fast', pause-resistant RNAP (33). However, the observation that gp39 accelerates *Tth* RNAP elongation (this work) and *E. coli* NusG accelerates *E. coli* RNAP elongation (6) to a similar extent suggests that the contribution of pausing to the overall elongation rate may be similar for both RNAPs.

It is instructive to contrast the antiterminating function of gp39 with those of λ proteins N and Q, two of the best-characterized transcription antiterminators, which also target the β flap domain, and p7, a regulatory protein from *X. oryzae* phage Xp10, which appears to be a functional analog of gp39 but binds RNAP near the

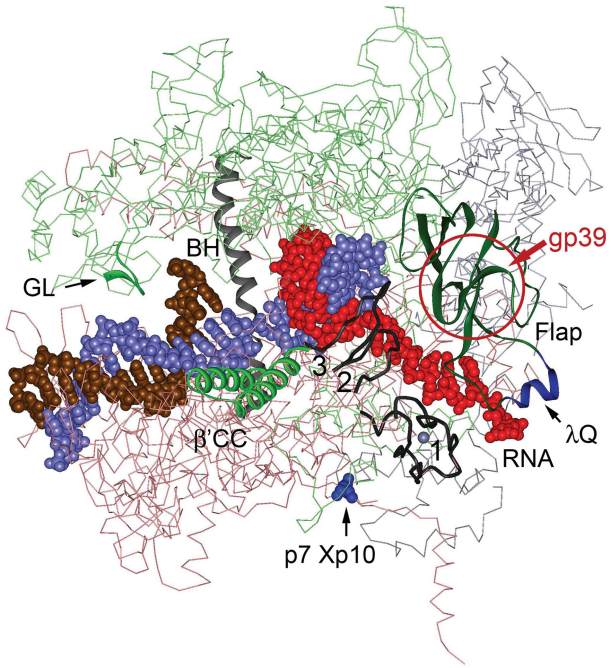

Figure 7. The binding sites of gp39 and other antiterminator proteins on the *Tth* RNAP TEC structure (21). The template and non-template DNA strands are shown in blue and brown, respectively, RNA is red. The β flap domain is dark green; the putative gp39-binding site is shown with red circle. β′ Zn finger [1], zipper [2] and lid [3] are shown as black lines. The proposed binding sites of the Xp10 p7 (β′ residue Glu4) and λ Q proteins (β flap tip helix) are shown in dark blue. The β′ coiled-coil (β′CC) and β gate-loop (GL) targeted by proteins of RfaH/NusG family are shown in green. The β′ bridge helix (BH) is gray.

β′ zinc finger domain located 'just below' the β flap, on the opposite side of the RNA exit channel (Figure 7). Three of the four proteins (excluding p7) were shown to stimulate transcription elongation and inhibit pausing, thus increasing the kinetic barrier to termination (9-11,32). Similar to the Q protein (40), gp39 significantly decreases the half-life of σ^{A}-dependent pauses, which are likely accompanied by RNAP backtracking, and reactivates paused TECs. Unlike gp39, the N and Q proteins also directly stabilize TECs during transcription through terminators (9,11,32). In particular, N and Q likely interfere with terminator hairpin formation, either by sequestering an upstream stem of the hairpin, as proposed for N (9), or by creating a 'shield' around the nascent RNA, as shown for Q^{82} (11). Finally, unlike N and Q, gp39 and p7 tightly bind their target RNAPs and do not require any *cis*-acting elements or additional factors such as NusA to convert RNAP into an antiterminating mode. In fact, both gp39 and p7 (41) appear to overcome the effects of NusA, a factor that by itself stimulates intrinsic termination, on transcription.

In conclusion, gp39 provides the first example of a phage-encoded transcription factor that affects all steps of transcription by bacterial RNAP and utilizes a simple antipausing mechanism for antitermination. Gp39 is small, binds tightly to *Thermus* RNAP and exhibits

robust effects on transcription. Thus, Gp39 is a highly attractive candidate for cocrystallization with *Thermus* RNAP in order to obtain the first molecular insights into the process of transcription antitermination.

SUPPLEMENTARY DATA

Supplementary Data are available at NAR Online: Supplementary Figures 1–8.

ACKNOWLEDGEMENTS

We thank I. Artsimovitch for plasmids and A. Hochschild for critical reading of the manuscript.

FUNDING

Russian Academy of Sciences Presidium Program in Molecular and Cellular Biology (grants to A.K. and K.S.); National Institutes of Health (NIH) (grant numbers R21 A1074769 to L.M. and R01 59295 to K.S.); the grant of the President of Russian Federation (MD-618.2011.4); Russian Foundation for Basic Research (10-04-00925); Federal Targeted Program 'Scientific and scientific-pedagogical personnel of innovative Russia 2009-2013' (state contracts 02.740.11.5132 and 02.740.11.0771); Pew Scholars Award (to B.E.N.). Funding for open access charge: NIH (grant R0159295).

Conflict of interest statement. None declared.

REFERENCES

1. Roberts,J.W., Shankar,S. and Filter,J.J. (2008) RNA polymerase elongation factors. *Annu. Rev. Microbiol.*, **62**, 211–233.
2. Peters,J.M., Vangeloff,A.D. and Landick,R. (2011) Bacterial transcription terminators: The RNA 3'-end chronicles. *J. Mol. Biol.*, **412**, 793–813.
3. Epshtein,V., Cardinale,C.J., Ruckenstein,A.E., Borukhov,S. and Nudler,E. (2007) An allosteric path to transcription termination. *Mol. Cell*, **28**, 991–1001.
4. Santangelo,T.J. and Artsimovitch,I. (2011) Termination and antitermination: RNA polymerase runs a stop sign. *Nat. Rev. Microbiol.*, **9**, 319–329.
5. Ha,K.S., Toulokhonov,I., Vassylyev,D.G. and Landick,R. (2010) The NusA N-terminal domain is necessary and sufficient for enhancement of transcriptional pausing via interaction with the RNA exit channel of RNA polymerase. *J. Mol. Biol.*, **401**, 708–725.
6. Herbert,K.M., Zhou,J., Mooney,R.A., Porta,A.L., Landick,R. and Block,S.M. (2010) E. coli NusG inhibits backtracking and accelerates pause-free transcription by promoting forward translocation of RNA polymerase. *J. Mol. Biol.*, **399**, 17–30.
7. Artsimovitch,I. and Landick,R. (2002) The transcriptional regulator RfaH stimulates RNA chain synthesis after recruitment to elongation complexes by the exposed nontemplate DNA strand. *Cell*, **109**, 193–203.
8. Svetlov,V., Belogurov,G.A., Shabrova,E., Vassylyev,D.G. and Artsimovitch,I. (2007) Allosteric control of the RNA polymerase by the elongation factor RfaH. *Nucleic Acids Res.*, **35**, 5694–5705.
9. Gusarov,I. and Nudler,E. (2001) Control of intrinsic transcription termination by N and NusA: the basic mechanisms. *Cell*, **107**, 437–449.
10. Rees,W.A., Weitzel,S.E., Das,A. and von Hippel,P.H. (1997) Regulation of the elongation-termination decision at intrinsic terminators by antitermination protein N of phage lambda. *J. Mol. Biol.*, **273**, 797–813.
11. Shankar,S., Hatoum,A. and Roberts,J.W. (2007) A transcription antiterminator constructs a NusA-dependent shield to the emerging transcript. *Mol. Cell*, **27**, 914–927.
12. Deighan,P., Diez,C.M., Leibman,M., Hochschild,A. and Nickels,B.E. (2008) The bacteriophage lambda Q antiterminator protein contacts the beta-flap domain of RNA polymerase. *Proc. Natl Acad. Sci. USA*, **105**, 15305–15310.
13. Yang,X., Molimau,S., Doherty,G.P., Johnston,E.B., Marles-Wright,J., Rothnagel,R., Hankamer,B., Lewis,R.J. and Lewis,P.J. (2009) The structure of bacterial RNA polymerase in complex with the essential transcription elongation factor NusA. *EMBO Rep.*, **10**, 997–1002.
14. Mooney,R.A., Schweimer,K., Rosch,P., Gottesman,M. and Landick,R. (2009) Two structuraly independent domains of E. coli NusG create regulatory plastisity via distinct interactions with RNA polymerase and regulators. *J. Mol. Biol.*, **391**, 341–358.
15. Sevostyanova,A., Svetlov,V., Vassylyev,D.G. and Artsimovitch,I. (2008) The elongation factor RfaH and the initiation factor sigma bind to the same site on the transcription elongation complex. *Proc. Natl Acad. Sci. USA*, **105**, 865–870.
16. Sevostyanova,A., Belogurov,G.A., Mooney,R.A., Landick,R. and Artsimovitch,I. (2011) The beta subunit gate loop is required for RNA polymerase modification by RfaH and NusG. *Mol. Cell*, **43**, 253–262.
17. Yuzenkova,Y., Zenkin,N. and Severinov,K. (2008) Mapping of RNA polymerase residues that interact with bacteriophage Xp10 transcription antitermination factor p7. *J. Mol. Biol.*, **375**, 29–35.
18. Zhang,G., Campbell,E.A., Minakhin,L., Richter,C., Severinov,K. and Darst,S.A. (1999) Crystal structure of *Thermus aquaticus* core RNA polymerase at 3.3 A resolution. *Cell*, **98**, 811–824.
19. Vassylyev,D.G., Sekine,S., Laptenko,O., Lee,J., Vassylyeva,M.N., Borukhov,S. and Yokoyama,S. (2002) Crystal structure of a bacterial RNA polymerase holoenzyme at 2.6 A resolution. *Nature*, **417**, 712–719.
20. Murakami,K.S., Masuda,S., Campbell,E.A., Muzzin,O. and Darst,S.A. (2002) Structural basis of transcription initiation: an RNA polymerase holoenzyme-DNA complex. *Science*, **296**, 1285–1290.
21. Vassylyev,D.G., Vassylyeva,M.N., Perederina,A., Tahirov,T.H. and Artsimovitch,I. (2007) Structural basis for transcription elongation by bacterial RNA polymerase. *Nature*, **448**, 157–162.
22. Berdygulova,Z., Westblade,L.F., Florens,L., Koonin,E.V., Chait,B.T., Ramanculov,E., Washburn,M.P., Darst,S.A., Severinov,K. and Minakhin,L. (2011) Temporal regulation of gene expression of the Thermus thermophilus bacteriophage P23-45. *J. Mol. Biol.*, **405**, 125–142.
23. Sevostyanova,A., Djordjevic,M., Kuznedelov,K., Naryshkina,T., Gelfand,M.S., Severinov,K. and Minakhin,L. (2007) Temporal regulation of viral transcription during development of Thermus thermophilus bacteriophage phiYS40. *J. Mol. Biol.*, **366**, 420–435.
24. Barinova,N., Kuznedelov,K., Severinov,K. and Kulbachinskiy,A. (2008) Structural modules of RNA polymerase required for transcription from promoters containing downstream basal promoter element GGGA. *J. Biol. Chem.*, **283**, 22482–22489.
25. Kuznedelov,K., Minakhin,L. and Severinov,K. (2003) Preparation and characterization of recombinant *Thermus aquaticus* RNA polymerase. *Methods Enzymol.*, **370**, 94–108.
26. Minakhin,L., Nechaev,S., Campbell,E.A. and Severinov,K. (2001) Recombinant *Thermus aquaticus* RNA polymerase, a new tool for structure- based analysis of transcription. *J. Bacteriol.*, **183**, 71–76.
27. Deaconescu,A.M., Chambers,A.L., Smith,A.J., Nickels,B.E., Hochschild,A., Savery,N.J. and Darst,S.A. (2006) Structural basis for bacterial transcription-coupled DNA repair. *Cell*, **124**, 507–520.
28. Nickels,B.E. (2009) Genetic assays to define and characterize protein-protein interactions involved in gene regulation. *Methods*, **47**, 53–62.

29. Thibodeau,S.A., Fang,R. and Joung,J.K. (2004) High-throughput beta-galactosidase assay for bacterial cell-based reporter systems. *Biotechniques*, **36**, 410–415.
30. Miropolskaya,N., Artsimovitch,I., Klimasauskas,S., Nikiforov,V. and Kulbachinskiy,A. (2009) Allosteric control of catalysis by the F loop of RNA polymerase. *Proc. Natl Acad. Sci. USA*, **106**, 18942–18947.
31. Dove,S.L. and Hochschild,A. (2004) A bacterial two-hybrid system based on transcription activation. *Methods Mol. Biol.*, **261**, 231–246.
32. Yarnell,W.S. and Roberts,J.W. (1999) Mechanism of intrinsic transcription termination and antitermination. *Science*, **284**, 611–615.
33. Sevostyanova,A. and Artsimovitch,I. (2010) Functional analysis of Thermus thermophilus transcription factor NusG. *Nucleic Acids Res.*, **38**, 7432–7445.
34. Ring,B.Z., Yarnell,W.S. and Roberts,J.W. (1996) Function of E. coli RNA polymerase sigma factor sigma 70 in promoter-proximal pausing. *Cell*, **86**, 485–493.
35. Perdue,S.A. and Roberts,J.W. (2011) Sigma(70)-dependent transcription pausing in Escherichia coli. *J. Mol. Biol.*, **412**, 782–792.
36. Toulokhonov,I., Artsimovitch,I. and Landick,R. (2001) Allosteric control of RNA polymerase by a site that contacts nascent RNA hairpins. *Science*, **292**, 730–733.
37. Toulokhonov,I. and Landick,R. (2003) The flap domain is required for pause RNA hairpin inhibition of catalysis by RNA polymerase and can modulate intrinsic termination. *Mol. Cell*, **12**, 1125–1136.
38. Landick,R. (2006) The regulatory roles and mechanism of transcriptional pausing. *Biochem. Soc. Trans.*, **34**, 1062–1066.
39. Sydow,J.F., Brueckner,F., Cheung,A.C., Damsma,G.E., Dengl,S., Lehmann,E., Vassylyev,D. and Cramer,P. (2009) Structural basis of transcription: mismatch-specific fidelity mechanisms and paused RNA polymerase II with frayed RNA. *Mol. Cell*, **34**, 710–721.
40. Marr,M.T. and Roberts,J.W. (2000) Function of transcription cleavage factors GreA and GreB at a regulatory pause site. *Mol. Cell*, **6**, 1275–1285.
41. Nechaev,S., Yuzenkova,Y., Niedziela-Majka,A., Heyduk,T. and Severinov,K. (2002) A novel bacteriophage-encoded RNA polymerase binding protein inhibits transcription initiation and abolishes transcription termination by host RNA polymerase. *J. Mol. Biol.*, **320**, 11–22.
42. Zhilina,E., Esyunina,D., Brodolin,K. and Kulbachinskiy,A. (2011) Structural transitions in the transcription elongation complexes of bacterial RNA polymerase during sigma-dependent pausing. *Nucl. Acids Res.*, December 2 (doi:10.1093/nar/gkr1158; epub ahead of print).